Supplementary Material for the Paper

"Faster Taylor Bubbles"

by Guangzhao Zhou & Andrea Prosperetti

Department of Mechanical Engineering, University of Houston

We carried out some preliminary simulations with a Galilei number $Ga = 5770$ and a Morton number $Mo = 2.5 \times 10^{-11}$, a value representative of water in the standard state. Due to time constraints, the simulations are somewhat under-resolved, but the results support those reported in the paper and are indicative of the trends to be expected for this larger value of Ga and smaller value of Mo.

With the physical parameters of water, the simulation corresponds to a round tube with an inner diameter of 15 mm; the cage diameter is 11.5 mm, the annulus width 1.78 mm and the rod diameter of 1.09 mm. The computed rise velocity of the bubble was 0.227 m/s to be compared with that predicted by the relation $0.351\sqrt{gD}$ which, with $D = 15$ mm, gives 0.135 m/s. The enhancement of the bubble rise velocity is therefore nearly 70% as in case A of the paper. The bubble Reynolds number (based on the cage diameter) is 2604. The bubble velocity exhibited some oscillations but was consistent with the previously quoted value (see figure 1). However, steady

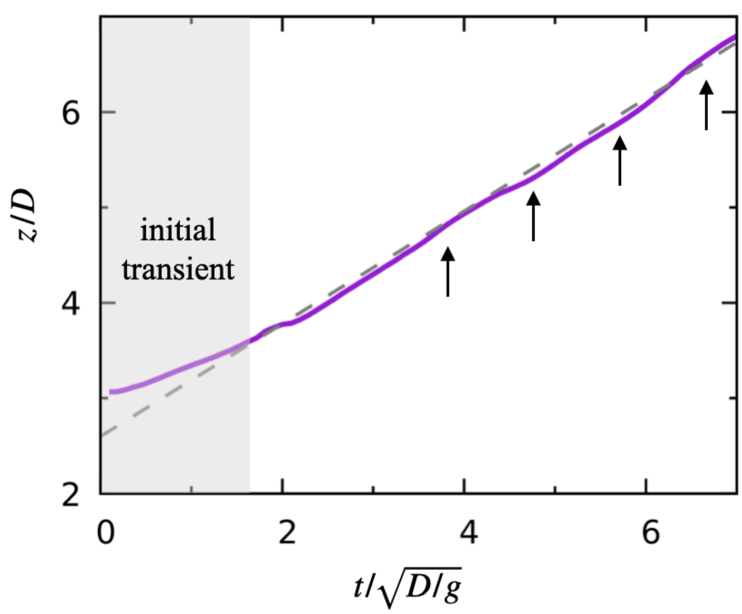

Figure 1: Position vs. time of the bubble tip. The dashed line corresponds to the (dimensional) velocity $U_B = 0.227$ m/s quoted in the text. The arrows indicate the instants at which the bubble shapes shown in figure 2 are taken.

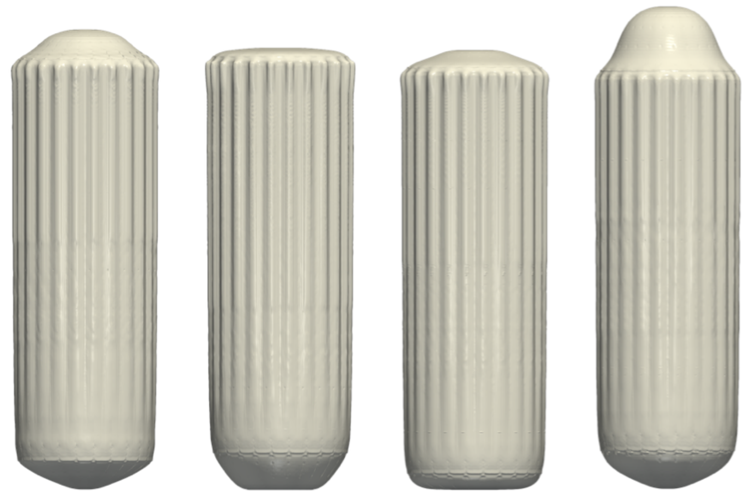

Figure 2: Probably due to the limited simulation time, in this simulation the bubble did not quite reach steady conditions but exhibited oscillations in the axial direction as shown here. The instants corresponding to the images shown are marked by arrows in figure 1.

conditions were not quite reached and the bubble exhibited shape oscillations in the axial direction, examples of which are shown in figure 2

Figure 3, to be compared with figure 4 in the paper, shows, from left to right, the pressure distribution, the vertical and horizontal liquid velocities and the bubble configuration at the instant

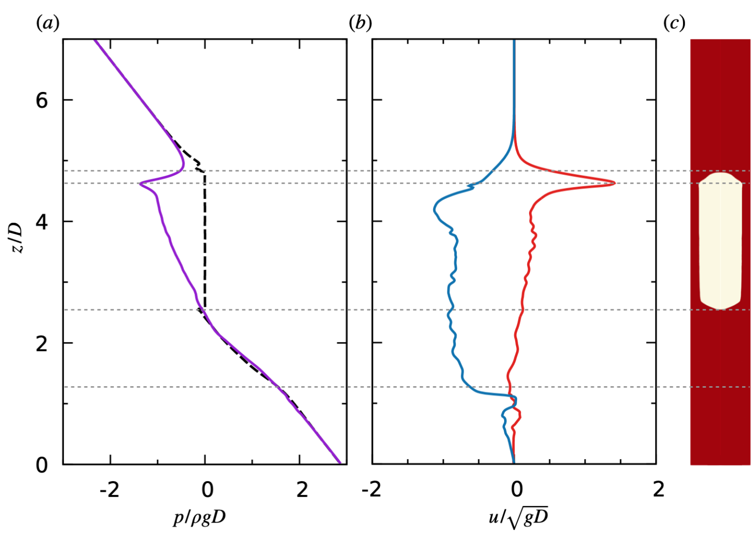

Figure 3: This figure is analogous to figure 4 in the paper and shows, from left to right, the pressure distribution, the vertical and horizontal liquid velocities and the bubble configuration at the instant these data are taken. The dashed line in panel (a) is the pressure along the axis of the tube, with the straight vertical portion the (constant) pressure in the bubble. The purple curve in (a) and the blue and red curves in (b) are taken along a line through the middle of the annulus.

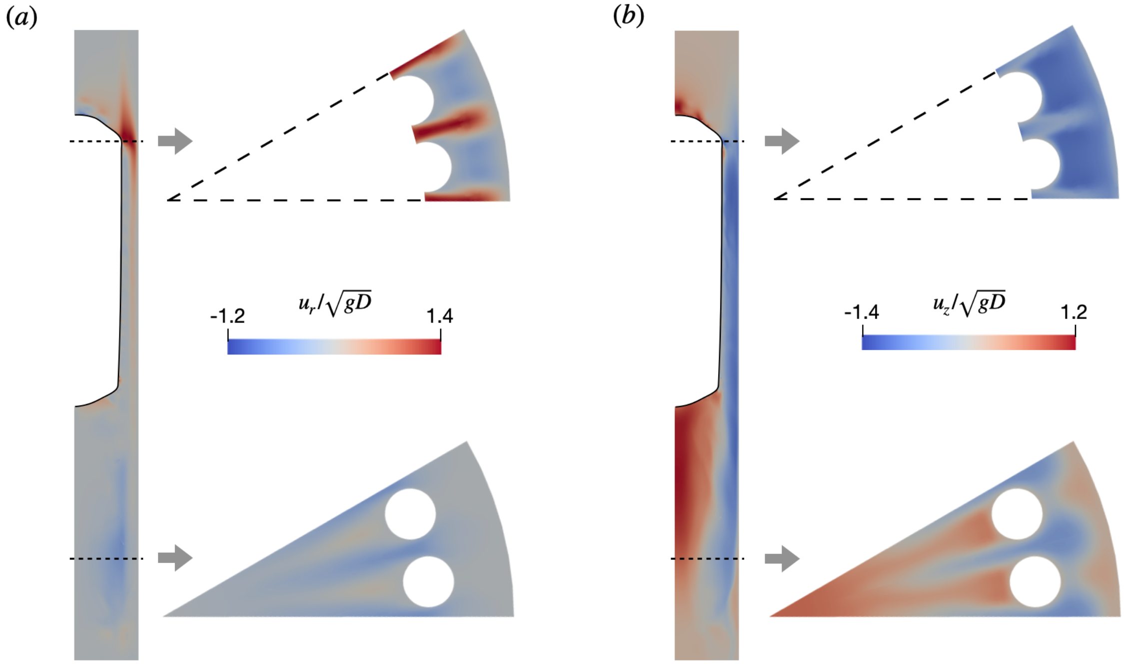

Figure 4: Color maps of the radial velocity, in (a), and of the vertical velocity, in (b) on vertical and horizontal planes. The latter are taken at the levels indicated by the arrows and the dotted lines.

these data are taken. The dashed line in panel (a) is the pressure along the axis of the tube, with the straight vertical portion the (constant) pressure in the bubble. The purple curve in (a) and the blue and red curves in (b) are taken along a line through the middle of the annulus. At the instant shown the transition zone toward the bubble tip is shortened which causes a faster outward flow into the annulus (red curve in (b)). The annulus-core pressure difference under the bubble is also significantly smaller than that shown in figure 4 of the paper. The negative vertical velocity extending well below the bubble in panel (b) indicates the presence of a long recirculating wake which delays the flow from the annulus back into the tube core. This is a well-known feature in high-Reynolds-number Taylor bubble flows. The waviness of the lines in panel (b) may perhaps be affected by the imperfect numerical resolution, but it must also be due to flow instabilities and unsteadiness since the Reynolds number of the flow in the annulus is about 560.

The color maps in figure 4, analogous to those of figure 5 in the paper, show the horizontal, in (a), and vertical, in (b), velocity distributions in a vertical plane and in two horizontal planes taken at the levels indicated by the arrows and dotted lines. Note in panel (a) the strong radial velocity issuing from the gap between the rods. This jet-like flow strikes the tube wall, where it splits into two streams which are carried downward by the flow in the annulus. The resulting streamlines take on a corkscrew appearance as shown in figure 5. The lower horizontal cut in panel (b) shows that, unlike the case of ordinary Taylor bubbles, the recirculating wake does not have axial symmetry but consists of lobes, corresponding to the position of the rods, separated by lower velocity streaks in correspondence of the radial inflow that can be seen in the lower horizontal cut of panel (a).

Some aspects of the complex flow in the annulus are illustrated in figure 5. Panel (a) gives a

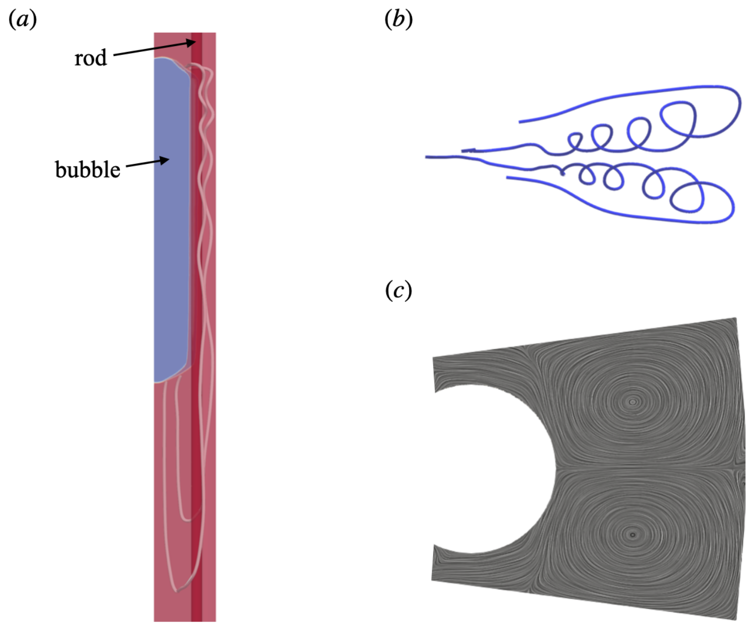

Figure 5: (a) Three-dimensional view of two streamlines in the computational domain. (b) Perspective view of the same streamlines from the above. (c) View from above of the vortices created in the annulus by the jet-like flow issuing from the gap between the rods.

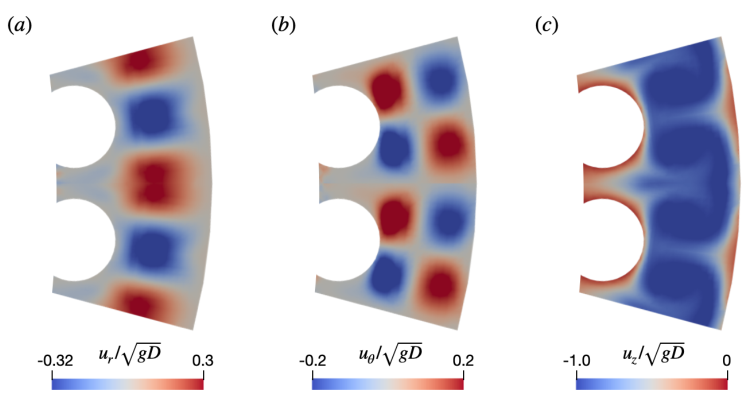

Figure 6: Color maps of the radial (a), azimuthal (b) and axial (c) velocities in a sector of the tube at the level of the middle of the bubble.

three-dimensional view of two streamlines. Panel (b) is a perspective view of the same streamlines in the annulus seen from above; the rods would be at the left end of the figure. Panel (c) is a view of the spiraling flow initiated in the annulus by the jet-like flow issuing from the gap between the rods at the top of the bubble; this view is taken at the middle of the bubble.

Color maps of the radial, azimuthal and vertical velocities at a level located at the middle of the bubble are shown in panels (a), (b) and (c) of figure 6. The radial velocity is positive opposite the gap and negative behind the rods. The azimuthal velocity exhibits the clover-leaf pattern characteristic of vortices (see figure 5). The vertical velocity is relatively large and downward.